Depression of Type I Diacylglycerol Kinases in Pancreatic β-Cells From Male Mice Results in Impaired Insulin Secretion

Yukiko Kurohane Kaneko, Yosuke Kobayashi, Keisuke Motoki, Kunihito Nakata, Shoko Miyagawa, Mao Yamamoto, Daiki Hayashi, Yasuhito Shirai, Fumio Sakane, and Tomohisa Ishikawa

Department of Pharmacology (Y.K.K., Y.K., K.M., K.N., S.M., T.I.), School of Pharmaceutical Sciences, University of Shizuoka, Shizuoka City 422–8526, Japan; Department of Applied Chemistry in Bioscience (M.Y., D.H., Y.S.), Graduate School of Agricultural Science, Faculty of Agriculture, Kobe University, Kobe 650–0017, Japan; and Department of Chemistry (F.S.), Graduate School of Science, Chiba University, Chiba 260–8670, Japan

Diacylglycerol kinase (DGK) catalyzes the conversion of diacylglycerol (DAG) to phosphatidic acid. This study investigated the expression and function of DGK in pancreatic β-cells. mRNA expression of type I DGK isoforms (α, β, γ) was detected in mouse pancreatic islets and the β-cell line MIN6. Protein expression of DGKα and DGKγ was also detected in mouse β-cells and MIN6 cells. The type I DGK inhibitor R59949 inhibited high K^+- and glucose-induced insulin secretion in MIN6 cells. Moreover, single knockdown of DGKα or DGKγ by small interfering RNA slightly but significantly decreased glucose- and high K^+-induced insulin secretions, and the double knockdown further decreased them to the levels comparable with those induced by R59949. R59949 and DiC8, a membrane permeable DAG analog, decreased intracellular Ca^{2+} concentration elevated by glucose and high K^+ in MIN6 cells. Real-time imaging in MIN6 cells expressing green fluorescent protein-tagged DGKα or DGKγ showed that the DGK activator phorbol 12-myristate 13-acetate rapidly induced translocation of DGKγ to the plasma membrane, whereas high K^+ slowly translocated DGKα and DGKγ to the plasma membrane. R59949 increased the DAG content in MIN6 cells when stimulated with high KCl, whereas it did not increase the DAG content but decreased the phosphatidic acid content when stimulated with high glucose. Finally, R59949 was confirmed to inhibit high K^+-induced insulin secretion from mouse islets and glucose-induced insulin secretion from rat islets. These results suggest that DGKα and DGKγ are present in β-cells and that the depression of these DGKs causes a decrease in intracellular Ca^{2+} concentration, thereby reducing insulin secretion. **(*Endocrinology* 154: 4089–4098, 2013)**

Type 2 diabetes is a chronic metabolic disorder that involves disruption of glucose and lipid metabolism. The disruption of diacylglycerol (DAG) metabolism is suggested to result in the progression of insulin resistance; the DAG metabolism induced by diacylglycerol kinase (DGK), which phosphorylates DAG to phosphatidic acid (PA), is deficient in skeletal muscle in type 2 diabetes (1). Defective glucose homeostasis also increased de novo DAG synthesis in pancreatic β-cells (2). Increased DAG production induces triacylglycerol production by DAG acyltransferase in β-cells, leading to β-cell dysfunction in type 2 diabetes (3).

DAG is also required for the normal functioning of β-cells. DAG concentrations increase in response to activation of glucose or muscarinic receptors in β-cells (4, 5). The primary role of DAG is to activate protein kinase C (PKC), which regulates insulin secretion (6) and β-cell apoptosis (7–9). In addition to the PKC-mediated pathway,

ISSN Print 0013-7227 ISSN Online 1945-7170
Printed in U.S.A.

Received April 17, 2013. Accepted September 5, 2013.
First Published Online September 13, 2013

Abbreviations: $[Ca^{2+}]_i$, intracellular Ca^{2+} concentration; DAG, diacylglycerol; DGK, diacylglycerol kinase; DiC8, 1,2-dioctanoyl-sn-glycerol; GFP, green fluorescent protein; HK buffer, HEPES-buffered Krebs-Ringer bicarbonate buffer; PA, phosphatidic acid; PKC, protein kinase C; PLC, phospholipase C; PLD, phospholipase D; PMA, phorbol 12-myristate 13-acetate; siRNA, small interfering RNA; VDCC, voltage-dependent Ca^{2+} channel.

DAG stimulates Ras guanyl nucleotide-releasing protein (10), protein kinase D (11), and transient receptor potential channels (12). In addition, DAG regulates insulin secretion in β-cells by regulating Munc13 independent of PKC activation (13).

PA is a bioactive lipid regulating cell growth and proliferation, membrane trafficking, and cytoskeletal reorganization (14). PA is generated in β-cells by glucose and muscarinic receptor activation and stimulates insulin secretion by increasing insulin granule traffic (15, 16). Thus, DAG and PA are both probably involved in the physiological regulation of insulin secretion from β-cells. The intracellular levels of these lipid messengers are strictly regulated by DGK, which terminates DAG signaling and initiates PA signaling.

To date, 10 mammalian DGK isoforms have been identified and divided into five groups based on their structure. Type I DGK isoforms, ie, DGKα, DGKβ, and DGKγ, have a pair of Ca^{2+}-binding EF-hand motifs, making these isoforms more active in the presence of Ca^{2+} (17). Recent studies have revealed that DGKα is highly expressed in T cells and acts during T cell activation and proliferation (18) and that DGKβ and DGKγ are abundantly expressed in rat brains and have functional roles in development of neurons (19). However, the role of DGK in β-cells has not been studied so far. Thus, the present study investigated the expression of type I DGK isoforms in β-cells and their effects on insulin secretion.

Materials and Methods

Animals

Male ddY mice weighing 35–45 g and male Wistar rats weighing 190–250 g (SLC) were used. The animals were housed in a 12-hour light, 12-hour dark cycle with food and water ad libitum. All experiments using laboratory animals in this study were performed with protocols approved by the Institutional Animal Care and Use Committee of the University of Shizuoka and according to the Guidelines for Animal Experiments established by the Japanese Pharmacological Society.

Isolation of mouse pancreatic islets

Pancreatic islets were isolated from male ddY mice and male Wistar rats using a collagenase digestion method. The solution used for the isolation was HEPES-buffered Krebs-Ringer bicarbonate buffer (HK buffer) containing 119 mM NaCl, 4.75 mM KCl, 5 mM $NaHCO_3$, 2.54 mM $CaCl_2$, 1.2 mM $MgSO_4$, 1.2 mM KH_2PO_4, and 10 mM HEPES (pH 7.4 adjusted with NaOH), supplemented with 2.8 mM glucose.

Cell culture and transfection

MIN6 cells (donated by Professor J.-I. Miyazaki, Osaka University, Osaka, Japan) were cultured in DMEM (Wako) supplemented with 100 U/mL penicillin, 100 μg/mL streptomycin, and 15% fetal bovine serum at 37°C in a humidified atmosphere of 95% air-5% CO_2. For the living cell imaging experiments, Lipofectamine 2000 (Invitrogen) reagents were used for transfection according to the manufacturer's instruction. In knockdown experiments, MIN6 cells were transfected with small interfering RNA (siRNA) by electroporation using a CLB-Transfection device (Lonza).

Reverse transcription-polymerase chain reaction

Freshly isolated mouse pancreatic islets and MIN6 cells were stored in RNA Later (QIAGEN) at −20°C. Total RNA was extracted from the islets and MIN6 cells using an RNeasy Total RNA kit (QIAGEN). Reverse transcription and PCR were performed using a One-Step RT-PCR kit (QIAGEN) with the gene-specific primers (*vide infra*). PCR fragments were separated by 2.0% agarose gel electrophoresis followed by staining with ethidium bromide.

The primers included the following: DGKα, forward, 5′-CTGGGCACTGGAAATGATCT-′, reverse, 5′-TCATGAGATGGAATCGGTGA-′; DGKβ, forward, 5′-CACACCCAACGACAAAGATG-′, reverse, 5′-CAGGTCGCTGAGAAGGTTTC-′; and DGKγ, forward, 5′-GAGCTGAAATGCTGTGTCCA-′, reverse, 5′-GGTGCCTGGTTTTTGTGAGT-′.

Immunoblotting

Freshly isolated mouse pancreatic islets or MIN6 cells were sonicated in ice-cold homogenization buffer consisting of 20 mM Tris-HCl (pH 7.4), 2 mM EDTA, 50 μg/mL phenylmethylsulfonylfluoride, 10 μg/mL aprotinin, 10 μg/mL leupeptin, and 250 mM sucrose. Protein samples were boiled in a buffer containing 62.5 mM Tris-HCl (pH 6.8), 2% sodium dodecyl sulfate, 10% glycerol, 5% 2-mercaptoethanol, and 0.0005% bromophenol blue. The samples were then separated on 10% or 14% polyacrylamide gel and transferred to a polyvinylidene difluoride membrane. The membrane was blocked with 5% skim milk in a buffer containing 10 mM Tris, 137 mM NaCl, and 0.1% Tween 20 and incubated overnight at 4°C with rabbit anti-DGKα (20), DGKβ (Abcam), or DGKγ antibody (21). After washing in the buffer containing 10 mM Tris, 137 mM NaCl, and 0.1% Tween 20, the membrane was further incubated with a horseradish peroxidase-conjugated donkey antirabbit IgG antibody (Cell Signaling Technology), and immunopositive bands were visualized with a commercialized kit (ECL plus Western blotting reagent pack; GE Healthcare; or Immunostar LD; WAKO Pure Chemical Industries).

Immunohistochemistry

Pancreata from male ddY mice were fixed with 3% paraformaldehyde and cryosectioned at 5 μm. The cryosections were blocked with 3% BSA (fraction V; Sigma-Aldrich) in PBS. They were incubated with guinea pig antiinsulin antibody (Dako) and rabbit anti-DGKα or DGKγ antibody (20, 21), followed by incubation with Alexa 488- or Alexa 546-conjugated secondary antibodies (Invitrogen). These samples were observed under fluorescence microscopy (BX51; Olympus).

Measurement of insulin secretion

MIN6 cells were preincubated in HK buffer with 0.1% BSA and 2.8 mM glucose for 1 hour at 37°C and then incubated for 1 hour with 2.8 or 22.2 mM glucose in the presence or absence

of drugs as indicated. Groups of five size-matched islets were preincubated in 1 mL of HK buffer with 0.1% BSA and 2.8 mmol/L glucose for 1 hour at 37°C. These islets were then incubated for 1 hour in various conditions. The incubation media were collected and stored at −20°C for later assay. The amount of insulin in the media was measured using an RIA kit (Eiken Chemical) or a rat insulin RIA kit (Millipore).

RNA interference experiments

siRNA against DGKα and DGKγ were purchased from QIAGEN.

DGKα siRNA sequences included the following: sense, 5′-GACAGAACAAAUAAACGAATT-3′, antisense, 5′-UUCG-UUUAUUUGUUCUGUCTG-3′; and DGKγ siRNA sequence, sense, 5′-GGAUGACGUUUCACCGCAATT-3′, antisense, 5′-UUGCGGUGAAACGUCAUCCGG-3′.

An unrelated control siRNA was also purchased from QIAGEN (AllStars Negative control siRNA). MIN6 cells were seeded 3 days before transfection and transfected with siRNA by electroporation using CLB-Transfection devices (Lonza), according to the manufacturer's protocol. The knockdown was confirmed by Western blotting and its efficiency was estimated by measuring the density of bands.

Measurement of intracellular Ca^{2+} concentration ($[Ca^{2+}]_i$)

MIN6 cells were plated onto coverslips and loaded with 4 μM fura PE3-AM for 2 hours at 37°C. The cells were then mounted on the stage of an inverted microscope in a chamber and continuously superfused with HK buffer containing 2.8 mM glucose and 0.1% BSA for 30 minutes at 37°C using a peristaltic pump at a flow rate of 1 mL/min. $[Ca^{2+}]_i$ was monitored at 510 nm emission wavelength with alternating excitation at 340 and 380 nm using the AQUACOSMOS/RATIO system (Hamamatsu Photonics). Fluorescence images obtained at 340 and 380 nm were captured in pairs at intervals of 10 seconds and converted to 340:380 ratio images after subtracting background fluorescence.

Live cell imaging

MIN6 cells were plated onto a glass-bottom dish and cultured for 48 hours. The cells were transfected with pEGFP-C3-DGKα or pEGFP-C3-DGKγ plasmid DNA using Lipofectamine 2000 reagent (Invitrogen). Forty-eight hours after transfection, the cells were analyzed by confocal microscopy (LSM510; Carl Zeiss).

The translocation index of DGK was quantified as described previously (22). Briefly, the averaged fluorescence intensity in an area including the plasma membrane [within 0.75 μm from the cell edge (Fp)] and whole cell (Fw) was measured by ImageJ software (National Institutes of Health). The relative translocation index was calculated by dividing Fp by Fw.

Measurement of PA and DAG

After 1×10^7 cells were treated with 22.2 mM glucose or 30 mM KCl in the absence and presence of 10 μM R59949 for 1 hour, the cells were harvested by centrifugation. The cell pellet was resuspended in 100 μL of 1 M NaCl and 20 μL of 1% perchloric acid, and lipids were extracted by 450 μL of chloroform-ethanol (1:2). After the addition of 150 μL of 1% perchloric acid and 150 μL of chloroform, the solvent phase was dried up. The total lipids including PA was resolved in 70 μL of 1% Triton X-100, and then the PA content was measured according to the method of Morita et al (23). The PA contents were normalized with protein concentration.

The amount of DAG was determined by its conversion into PA by *Escherichia coli* DGK by octyl glucoside mixed-micelle assay (24). Briefly, one third of the solvent phase described above was dried up with 200 μg of phosphsyifylserine (Sigma) and used as a substrate for the DGK assay. The reaction was performed for 10 minutes in the presence of [γ-^{32}P] ATP. The produced PA was separated on a 20-cm silica gel 60 TLC plate (Merck) using a chloroform-methanol-acetic acid (65:15:5) solution, and the radioactivity of PA was detected by BAS2500 (Fujix). The DAG contents were normalized with protein concentration.

Statistics

Results were expressed as mean ± SEM. Comparisons were made using a paired or unpaired *t* test or a Dunnett's multiple comparison test. $P < .05$ was considered significant.

Results

Expression of type I DGKs in mouse pancreatic islets and MIN6 cells

RT-PCR analysis showed that mRNAs of DGKα and DGKγ were highly expressed in mouse pancreatic islets and MIN6 cells. The mRNA expression of DGKβ was remarkably lower than that of other type I DGK isoforms. In addition, the protein expression of DGKα and DGKγ, but not DGKβ, was confirmed by Western blotting in mouse pancreatic islets and MIN6 cells (Figure 1). Moreover, immunostaining on mouse pancreatic sections showed that DGKα and DGKγ proteins were mainly expressed in the cytoplasm of pancreatic β-cells and exocrine cells (Figure 2).

Involvement of type I DGKs in insulin secretion in MIN6 cells

R59949, a specific inhibitor of type I DGKs (25, 26), inhibited glucose-induced insulin secretion from MIN6 cells in a concentration-dependent manner (Figure 3A). R59949 (10 μM) also inhibited insulin secretion induced by 30 mM K^+ at 2.8 mM glucose (Figure 3B). These results suggest that type I DGKs, ie, DGKα and DGKγ, are involved in insulin secretion.

The involvement of DGKα and DGKγ in insulin secretion was further investigated using siRNA. Suppression of DGKα and DGKγ expression was confirmed by Western blotting (Figure 4A). The knockdown efficiency of siRNAs for DGKα and DGKγ was 63% and 73%, respectively. Single knockdown of DGKα or DGKγ by siRNA slightly but significantly decreased insulin secretion induced by 22.2 mM glucose or 30 mM K^+ (Figure 4B).

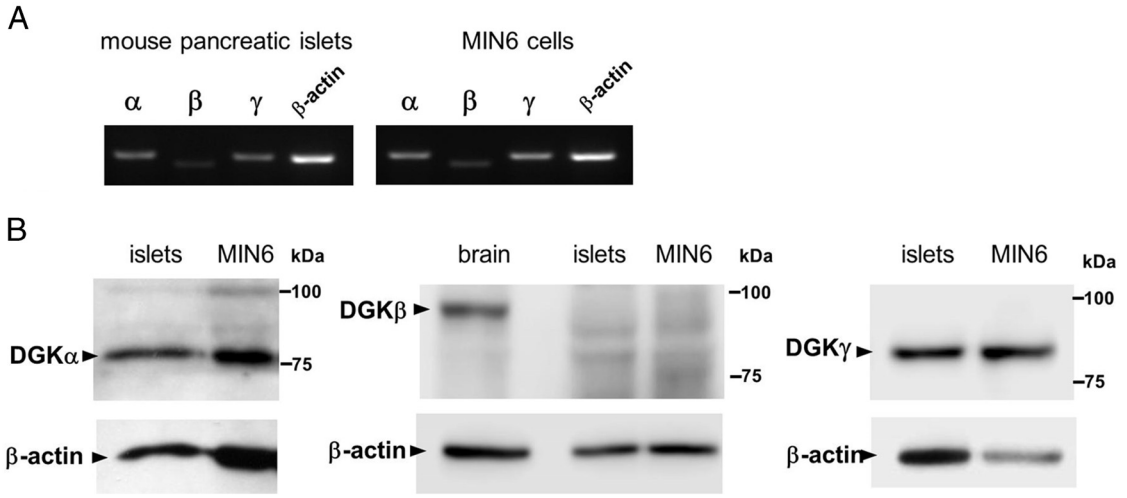

Figure 1. Identification of type I DGK isoforms in isolated mouse pancreatic islets and MIN6 cells. A, mRNA expression of DGKα, DGKβ, and DGKγ in mouse pancreatic islets and MIN6 cells was assessed by RT-PCR. B, Protein expression of DGKα, DGKβ, and DGKγ in mouse pancreatic islets and MIN6 cells was detected by Western blotting. A mouse brain homogenate was used as a positive control for DGKβ.

Double knockdown of DGKα and DGKγ by siRNA led to profound and significant decreases in insulin secretion induced by 22.2 mM glucose or 30 mM K^+ to the level comparable with those induced by R59949 (Figure 4B). The knockdown effects of DGKα and DGKγ on insulin secretion are likely to be additive. DGKα siRNA and DGKγ siRNA had no influence on the protein expression of DGKγ and DGKα, respectively (data not shown).

Involvement of type I DGKs in $[Ca^{2+}]_i$ responses of MIN6 cells

An intimate correlation is observed between $[Ca^{2+}]_i$ and insulin secretion in β-cells. We thus investigated the effect of R59949 on $[Ca^{2+}]_i$ elevation induced by 22.2 mM glucose. $[Ca^{2+}]_i$ of MIN6 cells was low and stable at 2.8 mM glucose. When the extracellular glucose concentration was increased to 22.2 mM, most MIN6 cells showed a transient $[Ca^{2+}]_i$ increase (first phase), followed by sustained $[Ca^{2+}]_i$ oscillations (second phase). R59949 induced an initial transient $[Ca^{2+}]_i$ elevation, followed by a significant decrease in $[Ca^{2+}]_i$, when applied at the second phase (Figure 5A). R59949 also largely suppressed the $[Ca^{2+}]_i$ elevation induced by high K^+ (30 mM) without any transient $[Ca^{2+}]_i$ increase (Figure 5B).

The inhibition of DGK is expected to lead to intracellular DAG accumulation. We thus investigated the effects of 1,2-dioctanoyl-sn-glycerol (DiC8), a membrane permeable DAG analog, on $[Ca^{2+}]_i$ elevation induced by 22.2 mM glucose or 30 mM K^+. As shown in Figure 5, C and D, DiC8 induced $[Ca^{2+}]_i$ responses comparable with those induced by R59949, suggesting that the $[Ca^{2+}]_i$ responses

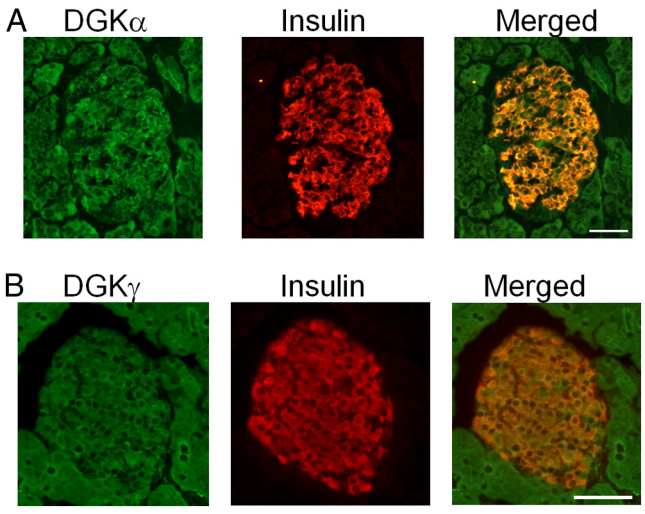

Figure 2. Distribution of DGKα and DGKγ in mouse pancreas. Frozen sections of mouse pancreas were immunostained with anti-DGKα (A, green) or DGKγ (B, green) and antiinsulin (red) antibodies. The right panels show the merged image. Bar, 50 μm.

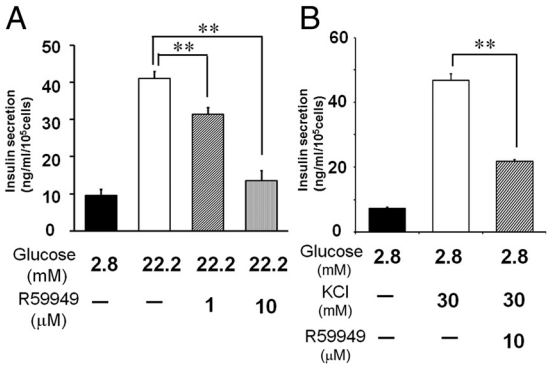

Figure 3. Effects of R59949, a type I DGK inhibitor, on glucose- and high K^+-induced insulin secretion in MIN6 cells. MIN6 cells were preincubated with or without R59949 for 30 minutes at 2.8 mM glucose and then incubated with or without 22.2 mM glucose (A) or 30 mM KCl (B) for 60 minutes. Each column represents the mean ± SEM of five to six experiments. **, $P < .01$.

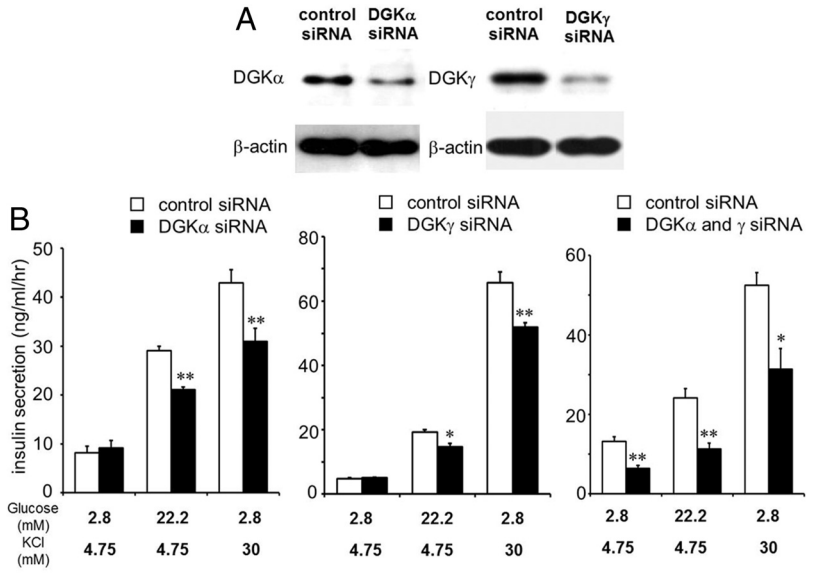

Figure 4. Effects of knockdown of DGKα and DGKγ on glucose- and high K^+-induced insulin secretion in MIN6 cells. A, Knockdown of DGKα and DGKγ by siRNA was confirmed by Western blotting. B, The effects of single knockdown of DGKα (left panel) or DGKγ (center panel) and double knockdown of DGKα and DGKγ (right panel) on insulin secretion induced by 22.2 mM glucose or 30 mM KCl. White columns, Control siRNA-transfected cells; black columns, DGKα and/or DGKγ siRNA-transfected cells. Each column represents the mean ± SEM of 4–14 experiments. *, $P < .05$, **, $P < .01$ vs corresponding control.

to the type I DGK inhibitor are mediated by DAG accumulation in β-cells.

Because DAG acts as a PKC activator, the possible involvement of PKC in the R59949- and DiC8-induced $[Ca^{2+}]_i$ responses was investigated. Ro31–8220 (1 μM), a PKC inhibitor, prevented only the initial $[Ca^{2+}]_i$ increase and had no effect on the sustained $[Ca^{2+}]_i$ decrease (Figure 5, E and F), suggesting that the initial $[Ca^{2+}]_i$ elevation is mediated by PKC activation, whereas the sustained $[Ca^{2+}]_i$ decrease is independent of PKC activation.

DGK activation in MIN6 cells

We investigated DGK activation in the MIN6 cells expressing green fluorescent protein (GFP)-tagged DGKα or DGKγ. The translocation of GFP-DGKs to the plasma membrane was used as an index of DGK activation (27). Phorbol 12-myristate 13-acetate (PMA), which is known to activate DGK as well as conventional and novel PKC, induced translocation of GFP-DGKγ to the plasma membrane within 15 seconds, which was sustained even after 15 minutes (Figure 6B, upper lane). In contrast, PMA had no effect on the intracellular distribution of GFP-DGKα (data not shown). When the cells were stimulated with high K^+ (30 mM), both DGKα and DGKγ were slowly translocated to the plasma membrane (Figure 6, A and B), which were restored to the cytosol after washout. However, the translocation of DGKα or DGKγ was not observed when the cells were stimulated with 22.2 mM glucose (data not shown). The translocation index of DGKα and DGKγ is shown in Figure 6C. DGKα and DGKγ were significantly translocated from cytosol to plasma membrane in the presence of high K^+.

Changes in DAG and PA contents by type I DGK inhibition

Table 1 shows the results of measuring DAG and PA contents in MIN6 cells. The stimulation with 22.2 mM glucose per se did not change the amounts of DAG and PA. The type I DGK inhibitor, R59949 (10 μM), did not change the DAG content but decreased the PA content when stimulated with 22.2 mM glucose. In contrast, the stimulation with 30 mM KCl per se lead to a small increase in DAG content and a small decrease in PA content; thereby the DAG to PA ratio was apparently increased. R59949 (10 μM) further increased DAG content in MIN6 cells stimulated with 30 mM KCl. Thus, R59949 was confirmed to induce the accumulation of DAG or the reduction of PA in MIN6 cells, which was, however, dependent on stimulators.

Involvement of type I DGKs in insulin secretion in mouse and rat islets

Finally, to confirm the results in MIN6 cells, we investigated the effect of the type I DGK inhibitor R59949 on insulin secretion. In isolated mouse islets, R59949 (30 μM) significantly inhibited 30 mM K^+-induced insulin secretion; however, the DGK inhibitor did not inhibit insulin secretion induced by 11.1 or 16.7 mM glucose (Figure 7A), which is not consistent with the results in MIN6 cells. We thus performed further experiments in isolated rat islets. Unlike in mouse islets, R59949 (10 μM) significantly inhibited insulin secretion induced by 11.1 mM glucose in rat islets (Figure 7B).

Discussion

This is the first report to demonstrate that DGKα and DGKγ are highly expressed and activated by $[Ca^{2+}]_i$ elevation in pancreatic β-cells. The results also suggest that DGKα and DGKγ act as a positive regulator of insulin secretion, which are probably mediated through preventing an excess accumulation of DAG in β-cells. We suggest

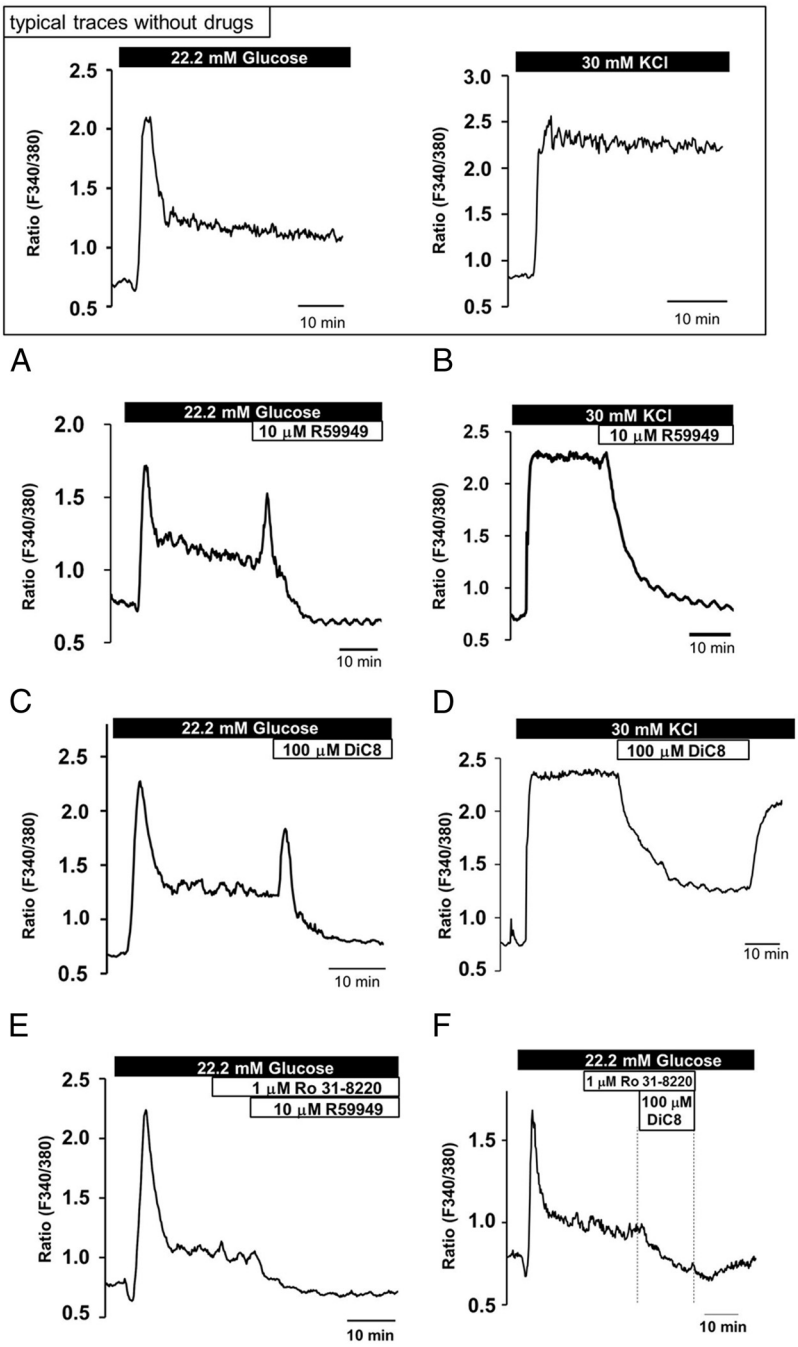

Figure 5. Effects of R59949 and DiC8, a membrane-permeable DAG analog, on glucose- and high K^+-induced elevation of $[Ca^{2+}]_i$ in MIN6 cells. MIN6 cells were perfused with HK buffer containing 2.8 mM glucose for more than 15 minutes before measuring $[Ca^{2+}]_i$. MIN6 cells were then perfused with HK buffer containing 22.2 mM glucose (A, C, E, and F) or 30 mM KCl (B and D). R59949 (10 μM; A, B, and E) or DiC8 (100 μM; C, D, and F) was applied to the perfusion solution in the absence and presence of the PKC inhibitor Ro31–8220 (1 μM; E and F), as indicated. The $[Ca^{2+}]_i$ responses to 22.2 mM glucose and 30 mM KCl without the drugs are shown in the top box. Tracings are representative results in 141 (A), 117 (B), 358 (C), 135 (D), 86 (E), and 55 cells (F) from two to six experiments.

The expression of DGKα and DGKγ was confirmed in the cytoplasm of mouse β-cells. The differential roles of DGKα and DGKγ have been proposed in other types of cells; DGKα acts as an antiapoptotic mediator and emerges as a multifaceted enzyme in T lymphocytes, whereas DGKγ acts as a negative regulator of Rac1 and as a positive regulator of cell cycle progression (28). In pancreatic β-cells, however, type I DGKs seem to play a similar role as a positive regulator of insulin secretion, which was supported by the present findings with the type I DGK inhibitor R59949 and the siRNA of DGKα and DGKγ. The involvement of type I DGKs in high K^+- and glucose-induced insulin secretion is also suggested by the experiments with R59949 in isolated mouse and rat islets, respectively, although R59949 showed no inhibitory effect on glucose-induced insulin secretion in mouse islets. This discrepancy in mouse islets may be explained by low expression of phospholipase Cδ, an isoform activated by Ca^{2+}, in mouse β-cells (vide infra).

DGK, which converts DAG to PA, acts as a terminator of DAG-mediated signals. The present results with the type I DGK inhibitor R59949 could therefore be interpreted that DAG accumulation is responsible for the inhibitory effects of R59949 on insulin secretion and $[Ca^{2+}]_i$ response. This notion is supported by the finding that the DAG analog DiC8 also inhibited high K^+-induced $[Ca^{2+}]_i$ elevation. These results are consistent with those of an early study by Thomas and Pek (29) in HIT-T15 β-cell lines, in which DiC8 and the DGK inhibitor R59022 inhibited high K^+-induced $[Ca^{2+}]_i$ elevation and insulin secretion. The present study further demonstrated that the inhibitory effects of R59949 and DiC8 were also caused when stimulated with glucose in MIN6 cells.

here that DGKα and DGKγ are activated in response to elevated $[Ca^{2+}]_i$ in β-cells and that hypoactivity of the DGKs leads to a pronounced suppression of $[Ca^{2+}]_i$ elevation, thereby leading to impaired insulin secretion.

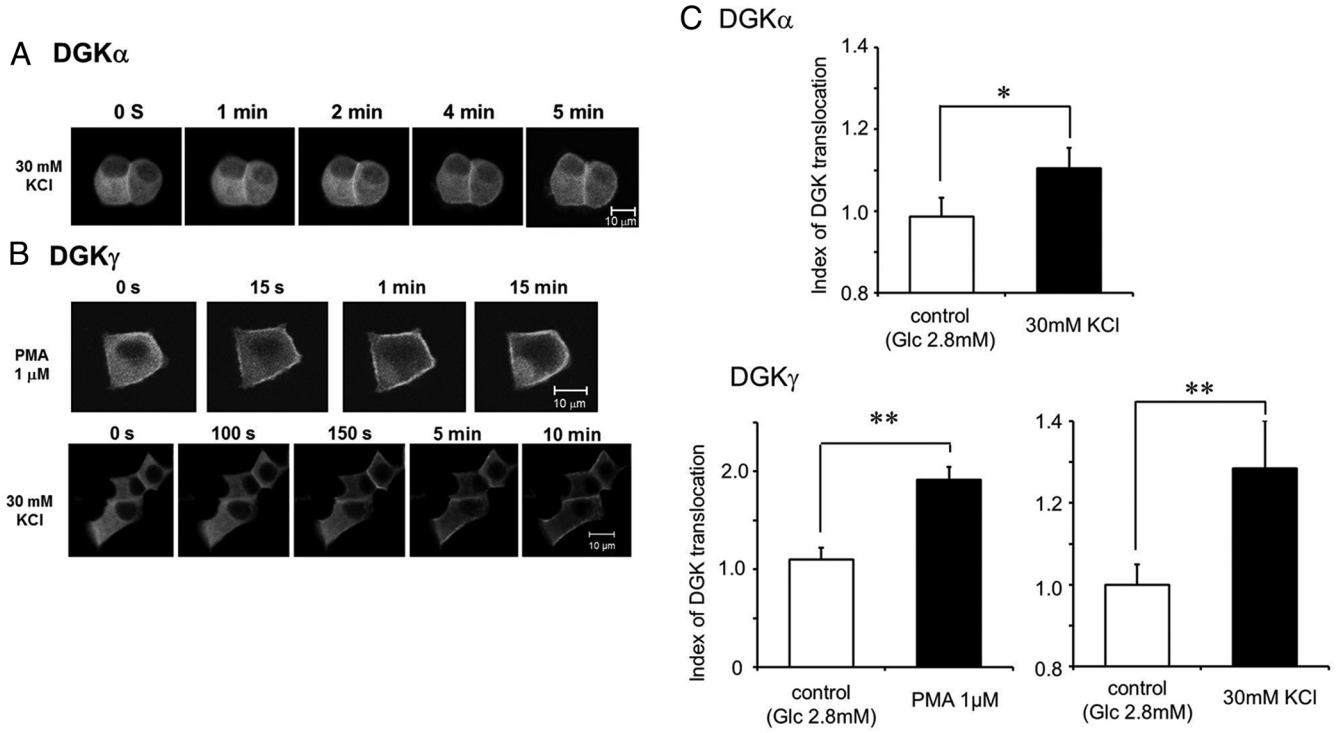

Figure 6. Translocation of DGKα and DGKγ in MIN6 cells. MIN6 cells were transfected with a plasmid encoding DGKα or DGKγ tagged with GFP. Bar, 10 μm. A, Application of 30 mM KCl induced GFP-DGKα translocation within 5 minutes. B, Upper lane, Application of 1 μM PMA quickly induced translocation of GFP-DGKγ within 15 seconds. Lower lane, Application of 30 mM KCl induced GFP-DGKγ translocation within 5 minutes. C, Statistical analysis was performed for the translocation of DGKα or DGKγ from the cytosol to the plasma membrane. The translocation was evaluated as described in *Material and Methods*. Each column represents the mean ± SEM of six to nine experiments. , *$P < .05$; **, $P < .01$.

R59949 declined $[Ca^{2+}]_i$ raised by glucose or high K^+. Thus, an accumulation of DAG resulting from type I DGK inhibition is suggested to inhibit Ca^{2+} influx through voltage-dependent Ca^{2+} channels (VDCC) because the $[Ca^{2+}]_i$ elevation induced by high K^+ and glucose was both totally abolished by nicardipine, a blocker of VDCC (data not shown). The mechanism for this is unclear at this time. Because VDCC is voltage-dependently activated, the inhibitory effects of DAG may be mediated by membrane hyperpolarization. However, it is less possible that DAG induces membrane hyperpolarization via activating some K^+ channels because R59949 or DiC8 markedly inhibited the $[Ca^{2+}]_i$ elevation induced by high K^+, in which the K^+ channel opening would have a little effect on membrane potential due to less K^+ gradient between the outside and the inside of the cell. Possible involvement of other mechanisms inducing membrane hyperpolarization may also be excluded because the inhibition of $[Ca^{2+}]_i$ by R59949 and DiC8 was remarkable. It is more likely, therefore, that DAG directly modulates channel activity of VDCC. A large amount of DAG is expected to alter the property of VDCC such as voltage dependency or conductivity because DAG could be incorporated into the cell membrane.

The accumulation of DAG was clearly confirmed when the cells were stimulated with 30 mM K^+ in the presence of R59949. DAG is thus suggested to be produced in response to the elevation of $[Ca^{2+}]_i$. The activation of phospholipase C (PLC) by glucose in islets has been shown to be regulated by Ca^{2+} (30, 31). Because the PLCδ1 isoform is more sensitive to Ca^{2+} compared with the other iso-

Table 1. Effects of the Type 1 DGK Inhibitor R59949 on the Amounts of DAG and PA in MIN6 Cells Stimulated by 22.2 mM Glucose or 30 mM K^+

	DAG	PA	DAG to PA Ratio
22.2 mM glucose	0.99 ± 0.10 (n = 7)	1.07 ± 0.03 (n = 7)	0.93
22.2 mM glucose + 10 μM R59949	1.03 ± 0.10 (n = 7)	0.78 ± 0.12 (n = 7)	1.32
30 mM KCl	1.12 ± 0.10 (n = 5)	0.87 ± 0.05 (n = 7)	1.29
30 mM KCl + 10 μM R59949	1.73 ± 0.09 (n = 5)[a]	0.93 ± 0.04 (n = 7)	1.87

Each value is expressed as a relative value to the basal value at glucose 2.8 mM. The ratio values of DAG to PA are also shown in the far right column.

[a] $P < .01$ vs corresponding control without R59949.

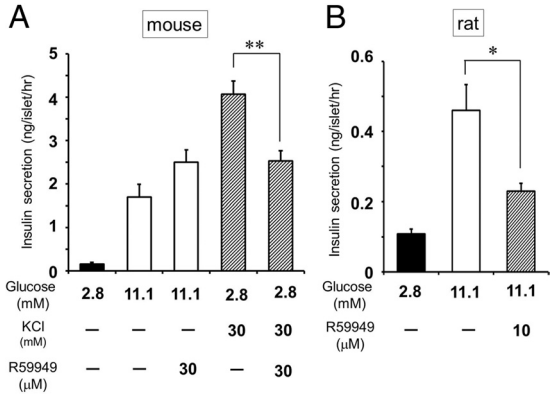

Figure 7. Effects of R59949 on glucose- and high K^+-induced insulin secretion in islets isolated from mice (A) and rats (B). Islets were preincubated with or without R59949 for 30 minutes at 2.8 mM glucose and then incubated with or without 11.1 mM glucose or 30 mM KCl for 60 minutes. Each column represents the mean ± SEM of five experiments. *, $P < .05$; **, $P < .01$.

forms and stimulated by an increase in $[Ca^{2+}]_i$ alone in the absence of any other activators (32), PLCδ1 is inferred to mediate the DAG production stimulated by high K^+ or glucose. Unexpectedly, however, the accumulation of DAG was not observed when MIN6 cells were stimulated with glucose. Several earlier studies have also failed to detect a glucose-induced increase in DAG in islets and β-cells (33, 34), which might be due to the transient nature of the increase in DAG induced by glucose stimulation (35). Even in the presence of R59949, DAG produced by glucose stimulation could be metabolized by DAG lipase. DAG is hydrolyzed by DAG lipase, giving rise to 2-arachidonylglycerol, which is, in turn, hydrolyzed to arachidonic acid by monoacylglycerol lipase (36). In fact, glucose has been shown to increase the level of arachidonic acid in islets (37). DAG produced by glucose stimulation of PLC may be rapidly metabolized to unesterized fatty acids. Although we failed to detect the accumulation of DAG in the response to glucose, the hypothesis that the DAG accumulation is responsible for the impaired insulin secretion induced by the inhibition of type I DGKs is still supported by other findings. A transient excess increase in DAG may be fully effective as a triggering signal for the impairment.

Insulin secretion induced by 30 mM K^+ was significantly suppressed by R59949 in mouse islets, which is consistent with the results in MIN6 cells, supporting the involvement of DGK in insulin secretion. Unfortunately, however, the notion was obscured by the unexpected finding that insulin secretion induced by glucose was insensitive to R59949. The results in mouse islets were further made complicated by the results in rat islets, which showed the inhibition by R59949 of insulin secretion induced by glucose. The difference between mouse and rat islets might be explained by the difference in the expression of PLC in β-cells. A study by Zawalich et al (38) has clearly demonstrated that the expression of PLCδ1, an isoform activated by Ca^{2+}, is much higher in rat islets than in mouse islets and that increases in PLC activity by glucose and high K^+ are larger in rat islets than in mouse islets. Thus, the DAG production by glucose could be estimated to be higher in the rat islets than in mouse islets; therefore, the inhibition by R59949 of glucose-induced insulin secretion might be observed only in rat islets.

The activation of DGKα and γ could be induced by an elevation of $[Ca^{2+}]_i$ because the translocation of these DGKs to the plasma membrane was observed when MIN6 cells were stimulated with high K^+. However, the translocation of DGKα or DGKγ was not detected when the cells were stimulated with 22.2 mM glucose. Because the insulin secretion induced by 22.2 mM glucose was reduced by the knockdown of DGKα and DGKγ by siRNA, DGKα and DGKγ are expected to be activated during glucose stimulation. High K^+ induced a sustained increase in $[Ca^{2+}]_i$, whereas 22.2 mM glucose induced a large $[Ca^{2+}]_i$ transient followed by a small oscillatory $[Ca^{2+}]_i$ elevation in MIN6 cells. Because DGKα and DGKγ seem to be activated by $[Ca^{2+}]_i$ elevation, the small $[Ca^{2+}]_i$ elevation during the sustained phase may have been insufficient to induce persistent DGKα and DGKγ translocation in MIN6 cells. Alternatively, repetitive translocation may not be easily detected by living cell imaging analysis in cells overexpressing GFP-fusion proteins.

The reduction of high K^+- and glucose-induced insulin secretions in the MIN6 cells with the single knockdown of DGKα or DGKγ by siRNA was relatively small compared with that with the type I DGK inhibitor R59949. The double knockdown of DGKα and DGKγ was required to reduce the insulin secretions to the level comparable with those induced by R59949. These results suggest that both DGKα and DGKγ participate in DAG metabolism during glucose stimulation and regulate insulin secretion. Hypofunction of either type I DGK may be compensated by the other.

Because DGK also acts as an activator of PA-mediated signals, part of the inhibition by R59949 may also result from a decrease in the intracellular PA level. The decrease in PA content was actually detected when MIN6 cells were stimulated with glucose in the presence of R59949. PA is produced through two major pathways: hydrolysis of phosphatidylcholine by phospholipase D (PLD) and phosphorylation of DAG by DGK. PLD and phospholipase C activities increase in response to glucose and other stimulants in pancreatic β-cells (38, 39). Moreover, PLD inhibition by butan-1-ol decreases glucose-induced insulin secretion, suggesting that PA is involved in glucose-in-

duced insulin secretion (39). Thus, PA is probably formed through the collaboration of DGK and PLD in β-cells. PA may promote the fusion of secretory vesicles by altering membrane curvature, as demonstrated in chromaffin cells (40). Moreover, upon stimulation of hepatocyte growth factor in epithelial cells, DGKα recruits and activates atypical PKCζ/ι at ruffling sites by producing PA, mediating the activation of Rac, a small G protein, and leading to the formation of membrane ruffles (41). PA has been shown to promote the trafficking and membrane association of Rac in β-cells (15). Collectively, PA produced by type I DGK possibly facilitates insulin secretion by accelerating exocytosis of insulin secretory granules in β-cells.

All mammalian DGKs have at least two cysteine-rich sequences homologous to the C1 domain of PKCs, in which the binding site for DAG and phorbol esters is located (18). In the present study, PMA induced translocation of DGKγ to the plasma membrane in β-cells but had no effect on intracellular distribution of DGKα. Similar results have been shown in CHO-K1 cells, in which another phorbol ester tetradecanoylphorbol 13-acetate induced translocation of DGKγ, but not DGKα, to the plasma membrane (27). These results are well correlated with sequence alignments performed by Hurley et al (42), who have divided C1 domain-containing proteins into two groups, typical and atypical, on the basis of fitting the consensus profile; C1 domains in the typical group fit the profile for phorbol ester binding, whereas those in the atypical do not. According to their classification, the C1 domains of DGKα are atypical, whereas one of the C1 domains, C1A domain, of DGKγ is typical. Thus, differential sensitivity to PMA between DGKα and DGKγ would be attributed to differences in the sequence of C1 domains.

DGK is functionally correlated with PKC. In skeletal muscle, glucose has been shown to activate DGK, thereby reducing conventional PKC activity (43). Although glucose activates the PLC/PKC pathway in pancreatic β-cells, the role of PKC in glucose-induced insulin secretion remains controversial. Several studies have shown that conventional PKC potentiates glucose-induced insulin secretion (44, 45), whereas others have suggested that conventional PKC is not involved (46, 47). Similarly, the effect of novel PKC on insulin secretion is also controversial (44, 46). In the present study, the type I DGK inhibitor R59949, which was expected to activate PKC through DAG accumulation, inhibited glucose- and high K^+-induced insulin secretion. However, PKC is unlikely to be involved in the inhibitory effect because the sustained inhibition of $[Ca^{2+}]_i$ elevation by R59949 or DiC8 was not affected by the PKC inhibitor Ro31–8220, although more detailed experiments would be required to conclude the involvement of PKC in the response to the inhibition of type I DGKs.

In summary, DGKα and DGKγ were shown to be present in pancreatic β-cells, be activated by $[Ca^{2+}]_i$ elevation, and participate in facilitation of insulin secretion. An excess accumulation of DAG, which occurs when DGKα and DGKγ are impaired, would cause a severe failure in insulin secretion. Targeting DAG or PA metabolism through the regulation of DGKα or DGKγ in β-cells may provide a novel therapeutic strategy to control impaired insulin secretion in type 2 diabetes.

Acknowledgments

Address all correspondence and requests for reprints to: Tomohisa Ishikawa, PhD, 52–1 Yada, Suruga-ku, Shizuoka City, Shizuoka 422–8526, Japan. E-mail: ishikat@u-shizuoka-ken.ac.jp.

This work was supported by Grants-in-Aid for Young Scientists (Grant 21790154, to Y.K.K.,) and Scientific Research (20590085, to T.I.) from the Japan Society for the Promotion of Science Grants-in-Aid for Scientific Research.

Disclosure Summary: The authors have nothing to disclose.

References

1. **Chibalin AV, Leng Y, Vieira E, et al.** Downregulation of diacylglycerol kinase δ contributes to hyperglycemia-induced insulin resistance. *Cell*. 2008;132:375–386.
2. **Delghingaro-Augusto V, Nolan CJ, Gupta D, et al.** Islet β cell failure in the 60% pancreatectomised obese hyperlipidaemic Zucker fatty rat: severe dysfunction with altered glycerolipid metabolism without steatosis or a falling beta cell mass. *Diabetologia*. 2009;52:1122–1132.
3. **Briaud I., Harmon JS, Kelpe CL, Segu VBG, Poitout V.** Lipotoxicity of the pancreatic β-cell is associated with glucose-dependent esterification of fatty acids into neutral lipids. *Diabetes*. 2001;50:315–321.
4. **Corkey BE, Glennon MC, Chen KS, Deeney JT, Matschinsky FM, Prentki M.** A role for malonyl-CoA in glucose-stimulated insulin secretion from clonal pancreatic β-cells. *J Biol Chem*. 1989;264:21608–21612.
5. **Peter-Riesch B, Fathi M, Schlegel W, Wollheim CB.** Glucose and carbachol generate 1, 2-diacylglycerols by different mechanisms in pancreatic islets. *J Clin Invest*. 1988;81:1154–1161.
6. **Uchida T, Iwashita N, Ohara-Imaizumi M, et al.** Protein kinase Cδ plays a non-redundant role in insulin secretion in pancreatic β cells. *J Biol Chem*. 2007;282:2707–2716.
7. **Eitel K, Staiger H, Rieger J, et al.** Protein kinase C δ activation and translocation to the nucleus are required for fatty acid-induced apoptosis of insulin-secreting cells. *Diabetes*. 2003;52:991–997.
8. **Wrede C, Dickson L, Lingohr M, Briaud I, Rhodes C.** Fatty acid and phorbol ester-mediated interference of mitogenic signaling via novel protein kinase C isoforms in pancreatic β-cells (INS-1). *J Mol Endocrinol*. 2003;30:271–286.
9. **Hennige AM, Ranta F, Heinzelmann I, et al.** Overexpression of kinase-negative protein kinase Cδ in pancreatic β-cells protects mice from diet-induced glucose intolerance and β-cell dysfunction. *Diabetes*. 2010;59:119–127.

10. **Ebinu JO, Bottorff DA, Chan EYW, Stang SL, Dunn RJ, Stone JC.** RasGRP, a Ras guanyl nucleotide-releasing protein with calcium- and diacylglycerol-binding motifs. *Science*. 1998;280:1082–1086.
11. **Baron CL, Malhotra V.** Role of diacylglycerol in PKD recruitment to the TGN and protein transport to the plasma membrane. *Science*. 2002;295:325–328.
12. **Hofmann T, Obukhov AG, Schaefer M, Harteneck C, Gudermann T, Schultz G.** Direct activation of human TRPC6 and TRPC3 channels by diacylglycerol. *Nature*. 1999;397:259–263.
13. **Rhee JS, Betz A, Pyott S, et al.** β Phorbol ester- and diacylglycerol-induced augmentation of transmitter release is mediated by Munc13s and not by PKCs. *Cell*. 2002;108:121–133.
14. **Zhang Y, Du G.** Phosphatidic acid signaling regulation of Ras superfamily of small guanosine triphosphatases. *Biochim Biophys Acta*. 2009;1791:850–855.
15. **McDonald P, Veluthakal R, Kaur H, Kowluru A.** Biologically active lipids promote trafficking and membrane association of Rac1 in insulin-secreting INS 832/13 cells. *Am J Physiol Cell Physiol*. 2007; 292:C1216–C1220.
16. **Farese RV, DiMarco PE, Barnes DE, et al.** Rapid glucose-dependent increases in phosphatidic acid and phosphoinositides in rat pancreatic islets. *Endocrinology*. 1986;118:1498–1503.
17. **Yamada K, Sakane F, Matsushima N, Kanoh H.** EF-hand motifs of α, β and γ isoforms of diacylglycerol kinase bind calcium with different affinities and conformational changes. *Biochem J*. 1997;321: 59–64.
18. **Mérida I, Ávila-Flores A, Merino E.** Diacylglycerol kinases: at the hub of cell signaling. *Biochem J*. 2008;409:1–18.
19. **Adachi N, Oyasu M, Taniguchi T, et al.** Immunocytochemical localization of a neuron-specific diacylglycerol kinase β and γ in the developing rat brain. *Mol Brain Res*. 2005;139:288–299.
20. **Goto K, Watanabe M, Kondo H, Yuasa H, Sakane F, Kanoh H.** Gene cloning, sequence, expression and in situ localization of 80-kDa diacylglycerol kinase specific to oligodendrocyte of rat brain. *Mol Brain Res*. 1992;16:75–87.
21. **Matsubara T, Shirai Y, Miyasaka K, et al.** Nuclear transportation of diacylglycerol kinase γ and its possible function in the nucleus. *J Biol Chem*. 2006;281:6152–6164.
22. **Yagi K, Shirai Y, Hirai M, Sakai N, Saito N.** Phospholipase A2 products retain a neuron specific γ isoform of PKC on the plasma membrane through the C1 domain—a molecular mechanism for sustained enzyme activity. *Neurochem Int*. 2004;45:39–47.
23. **Morita SY, Ueda K, Kitagawa S.** Enzymatic measurement of phosphatidic acid in cultured cells. *J Lipid Res*. 2009;50:1945–1952.
24. **Sakane F, Imai S, Kai M, Wada I, Kanoh H.** Molecular cloning of a novel diacylglycerol kinase isozyme with a pleckstrin homology domain and a C-terminal tail similar to those of the EPH family of protein-tyrosine kinases. *J Biol Chem*. 1996;271:8394–8401.
25. **de Chaffoy de Courcelles D, Roevens P, Van Belle H, Kennis L, Somers Y, De Clerck F.** The role of endogenously formed diacylglycerol in the propagation and termination of platelet activation. A biochemical and functional analysis using the novel diacylglycerol kinase inhibitor, R 59949. *J Biol Chem*. 1989;264:3274–3285.
26. **Jiang Y, Sakane F, Kanoh H, Walsh JP.** Selectivity of the diacylglycerol kinase inhibitor 3-{2-(4-[bis-(4-fluorophenyl)methylene]-1-piperidinyl)ethyl}-2,3-dihydro-2-thioxo-4(1H)quinazolinone (R59949) among diacylglycerol kinase subtypes. *Biochem Pharmacol*. 2000;59:763–772.
27. **Shirai Y, Segawa S, Kuriyama M, Goto K, Sakai N, Saito N.** Subtype-specific translocation of diacylglycerol kinase α and γ and its correlation with protein kinase C. *J. Biol. Chem*. 2000;275:24760–24766.
28. **Sakane F, Imai S, Kai M, Yasuda S, Kanoh H.** Diacylglycerol kinases: why so many of them? *Biochim Biophys Acta*. 2007;1771:793–806.
29. **Thomas TP, Pek SB.** Diacylglycerol inhibits potassium-induced calcium influx and insulin release by a protein kinase-C-independent mechanism in HIT T-15 islet cells. *Endocrinology*. 1992;131:1985–1992.
30. **Axen KV, Schubart UK, Blake AD, Fleischer N.** Role of Ca^{2+} in secretagogue-stimulated breakdown of phosphatidylinositol in rat pancreatic islets. *J Clin Invest*. 1983;72:13–21.
31. **Zawalich WS, Diaz VA, Zawalich KC.** Influence of cAMP and calcium on [^{3}H]inositol efflux, inositol phosphate accumulation, and insulin release from isolated rat islets. *Diabetes*. 1988;37:1478–1483.
32. **Katan M.** Families of phosphoinositide-specific phospholipase C: structure and function. *Biochim Biophys Acta*. 1998;1436:5–17.
33. **Regazzi R, Li GD, Deshusses J, Wollheim CB.** Stimulus-response coupling in insulin-secreting HIT cells. Effects of secretagogues on cytosolic Ca^{2+}, diacylglycerol, and protein kinase C activity. *J Biol Chem*. 1990;265:15003–15009.
34. **Wolf BA, Easom RA, McDaniel ML, Turk J.** Diacylglycerol synthesis de novo from glucose by pancreatic islets isolated from rats and humans. *J Clin Invest*. 1990;85:482–490.
35. **Dunlop ME, Larkins RG.** Activity of endogenous phospholipase C and phospholipase A_2 in glucose stimulated pancreatic islets. *Biochem Biophys Res Commun*. 1984;120:820–827.
36. **Konrad RJ, Major CD, Wolf BA.** Diacylglycerol hydrolysis to arachidonic acid is necessary for insulin secretion from isolated pancreatic islets: sequential actions of diacylglycerol and monoacylglycerol lipases. *Biochemistry*. 1994;33:13284–13294.
37. **Wolf BA, Turk J, Sherman WR, McDaniel ML.** Intracellular Ca^{2+} mobilization by arachidonic acid. Comparison with myo-inositol 1,4,5-trisphosphate in isolated pancreatic islets. *J Biol Chem*. 1986; 261:3501–3511.
38. **Zawalich WS, Bonnet-Eymard M, Zawalich KC.** Insulin secretion, inositol phosphate levels, and phospholipase C isozymes in rodent pancreatic islets. *Metabolism*. 2000;49:1156–1163.
39. **Hughes WE.** Phospholipase D1 regulates secretagogue-stimulated insulin release in pancreatic β-cells. *J Biol Chem*. 2004;279:27534–27541.
40. **Bader M-F, Vitale N.** Phospholipase D in calcium-regulated exocytosis: lessons from chromaffin cells. *Biochim Biophys Acta*. 2009; 1791:936–941.
41. **Chianale F, Rainero E, Cianflone C, et al.** Diacylglycerol kinase α mediates HGF-induced Rac activation and membrane ruffling by regulating atypical PKC and RhoGDI. *Proc Natl Acad Sci USA*. 2010;107:4182–4187.
42. **Hurley JH, Newton AC, Parker PJ, Blumberg PM, Nishizuka Y.** Taxonomy and function of C1 protein kinase C homology domains. *Protein Sci*. 1997;6:477–480.
43. **Miele C, Paturzo F, Teperino R, et al.** Glucose regulates diacylglycerol intracellular levels and protein kinase C activity by modulating diacylglycerol kinase subcellular localization. *J Biol Chem*. 2007; 282:31835–31843.
44. **Warwar N, Efendic S, Östenson C-G, Haber EP, Cerasi E, Nesher R.** Dynamics of glucose-induced localization of PKC isoenzymes in pancreatic β-cells. *Diabetes*. 2006;55:590–599.
45. **Yedovitzky M, Mochly-Rosen D, Johnson JA, et al.** Translocation inhibitors define specificity of protein kinase C isoenzymes in pancreatic β-cells. *J Biol Chem*. 1997;272:1417–1420.
46. **Carpenter L, Mitchell CJ, Xu ZZ, Poronnik P, Both, GW, Biden TJ.** PKCα is activated but not required during glucose-induced insulin secretion from rat pancreatic islets. *Diabetes*. 2004;53:53–60.
47. **Schmitz-Peiffer C, Biden TJ.** Protein kinase C function in muscle, liver, and β-cells and its therapeutic implications for type 2 diabetes. *Diabetes*. 2008;57:1774–1783.